

# 1 COVID-19 and urban exodus: diverging population redistribution patterns across countries 2 from 2020 to 2022

3 Qianwen Duan <sup>a\*</sup>, Shengjie Lai <sup>b</sup>, Alessandro Sorichetta <sup>c</sup>, Andrew J. Tatem <sup>b</sup>, Jessica Steele <sup>b</sup>, Felix Eigenbrod <sup>a</sup>

4 <sup>a</sup> School of Geography and Environmental Science, University of Southampton, Southampton SO17 1BJ, United  
5 Kingdom

6 <sup>b</sup> WorldPop, School of Geography and Environmental Science, University of Southampton, Southampton SO17  
7 1BJ, United Kingdom

8 <sup>c</sup> Dipartimento di Scienze della Terra “Ardito Desio”, Università degli Studi di Milano, Via Mangiagalli 34, 20133  
9 Milan, Italy

10 \* Corresponding author: Qianwen Duan [Q.Duan@soton.ac.uk](mailto:Q.Duan@soton.ac.uk)

11

## 12 Abstract

13 While widespread urbanisation continues, emerging trends of population redistribution away from  
14 highly urbanised areas have been observed in some countries, with important implications for  
15 infrastructure planning, resource allocation, and environmental risk assessment. However, few  
16 studies have examined this trend in a timely and spatially comprehensive manner across diverse  
17 national contexts, particularly in response to the turbulence in migration patterns caused by the  
18 COVID-19 pandemic. Here, we analyse spatial Facebook population data from 2020 to 2022 across 35  
19 countries to characterise two forms of population redistribution: shifts between urban and rural  
20 areas, and changes along the urban density gradient. During the early response phase of the  
21 pandemic, broader country-level trends of urban-to-rural redistribution and intra-urban  
22 deconcentration were evident. However, 20% and 4.8% of these trends, respectively, were  
23 temporary and reversed during the later phase of the pandemic. The extent and direction of these  
24 patterns varied across countries and were negatively associated with the Human Development Index,  
25 suggesting that developed nations experienced greater urban depopulation and spatial  
26 deconcentration. Our findings reveal a potential misalignment between population redistribution  
27 and existing physical urban densities in certain countries, as densely built-up areas are experiencing  
28 outflows, highlighting the need for adaptive urban planning strategies to address evolving population  
29 dynamics and related sustainability challenges.

30

## 31 Introduction

32 Our world has experienced rapid urbanisation over the past few decades. From 1960 to 2020, the  
33 urban population increased from 1.0 to 4.4 billion, with over 50% of inhabitants living in urban areas  
34 <sup>1</sup>. In general, this increasing trend is widely expected to continue <sup>2</sup>. However, a contrasting  
35 phenomenon of urban depopulation has occurred in some countries, particularly in the Global  
36 North, where populations are relocating to less urbanised areas <sup>3,4</sup>. Although this shift may remain  
37 modest and in its early stages compared to the dominant trend of urban growth<sup>5</sup>, it may signal long-  
38 term changes. It is predicted that half of US cities will experience population loss by 2100 <sup>6</sup>. More  
39 recently, the COVID-19 pandemic and interventions triggered an unprecedented global shock to  
40 migration patterns <sup>7,8</sup>. Lockdowns, fear of COVID-19 spread, and shifts in lifestyle such as the rise of  
41 remote work led many people to reconsider their living environments, sparking a growing interest in  
42 less urbanised areas during the pandemic <sup>9,10</sup>. These shifts raise important questions about the

43 future of urbanisation and whether the traditional assumption of ever-growing populations in cities  
44 needs to be reconsidered.

45 Understanding changes in population distributions across varying urbanised areas is important for  
46 various fields, from infrastructure planning<sup>6,11</sup> to resource allocation<sup>12</sup> and environmental risk  
47 assessment<sup>13–15</sup>. Most past planning assumed that urban populations would continually grow<sup>7</sup>. Our  
48 research aims to explore whether this trend is shifting, particularly in response to the shock of  
49 COVID-19, and highlights the need to adapt future planning accordingly. For example, highly  
50 urbanised areas experiencing population declines may no longer require extensive construction and  
51 investment due to existing underutilised infrastructure and should instead focus on maintaining  
52 them<sup>6,16</sup>. Conversely, rural and peri-urban areas facing an influx of new residents may require  
53 enhanced public services and transportation networks. Meanwhile, the reshaping of derelict land in  
54 depopulated built areas<sup>6</sup>, alongside the revitalisation of landscapes in areas with increased  
55 population<sup>13</sup>, presents new environmental opportunities and challenges.

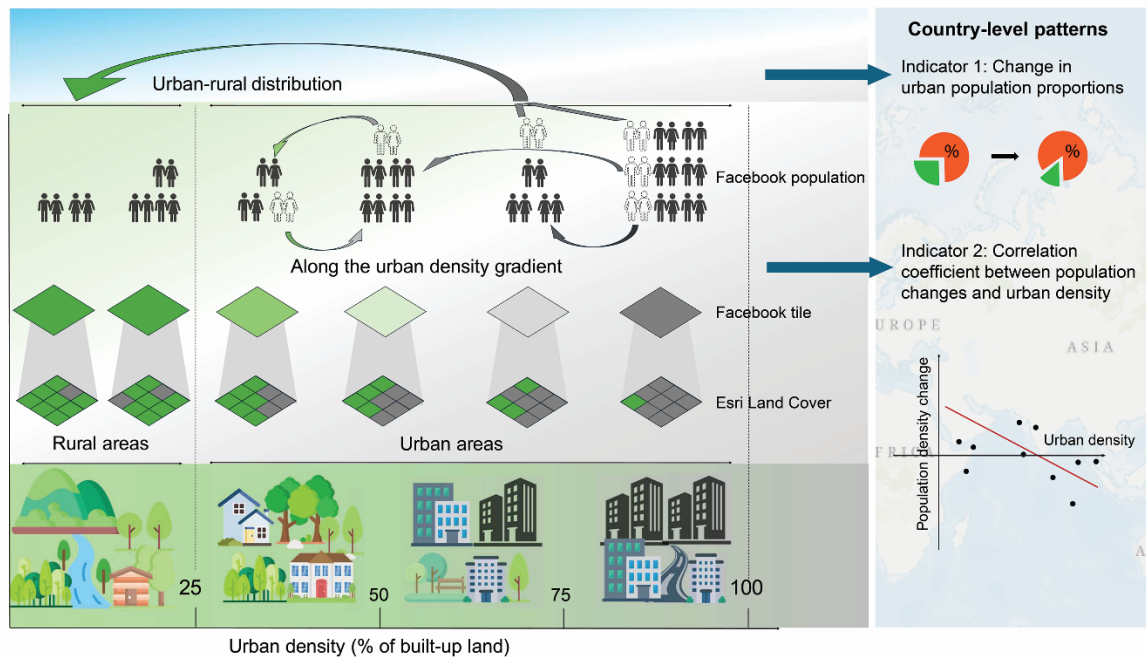
56 However, traditional data sources often fall short in capturing timely and spatially detailed  
57 population changes. Spatial population maps, which usually allocate populations based on layers  
58 including satellite imagery-derived settlement extents and land cover types, do not accurately  
59 provide real-time population shifts and migration patterns within those extents<sup>17</sup>. Recently, the  
60 growing availability of mobile phone location data from the Global Positioning System (GPS) and  
61 online social media and smartphone applications of digital platforms, such as Google<sup>18</sup>, Apple<sup>19</sup> and  
62 Meta (Facebook)<sup>20–22</sup>, provides new opportunities to better understand near-real-time population  
63 distributions across space and time, although user representation biases exist. For example,  
64 Facebook data derived from aggregated user location history have been used to assess population  
65 exposure to climate risks and monitor density changes during disasters and emergencies<sup>23–25</sup>. During  
66 the COVID-19 pandemic in particular, these data were invaluable for tracking mobility patterns<sup>22,26</sup>  
67 and urban–rural shifts<sup>20,27–29</sup>. Yet, most existing studies using such data to examine urban–rural shifts  
68 have focused on individual countries or regions<sup>27,30,31</sup> due to limited data access, leaving little  
69 understanding of the common characteristics underlying patterns of population redistribution in  
70 different socio-economic settings. Additionally, while the pandemic might have influenced shifts in  
71 population distribution, it remains unclear whether these changes were merely temporary.

72 In this study, we seek to answer two questions: 1) how has population distribution across various  
73 urbanised areas changed during COVID-19 across different countries; 2) what socioeconomic  
74 characteristics were associated with the heterogeneity in country-level population redistribution  
75 patterns. Using spatially referenced Facebook population data from Meta<sup>21</sup> during night-time and  
76 following a recently developed pre-processing approach<sup>20</sup> (see Methods), we analysed trends in  
77 population distribution from 2020 to 2022 across varying urbanised areas in 35 countries (23 high-  
78 income and 12 middle-income). Physical urban density (% of built-up areas; Supplementary Fig. 3)  
79 was used to characterise degrees of urbanisation, and is considered to be closely linked to  
80 infrastructure distribution<sup>32,33</sup>. Our findings provide valuable insights into both cross-national and  
81 fine-grained patterns of population redistribution in response to COVID-19, and also contribute to a  
82 broader understanding of urban–rural continuum dynamics, highlighting the importance of adaptive  
83 urban planning, policy, and resource management in a post-pandemic world.

84

## 85 **Results**

86 For each country, we analysed population redistribution patterns by examining changes in urban-  
 87 rural distribution and along the urban density gradient. To quantify these patterns at the country  
 88 level, we calculated two indicators separately: (1) the change in urban population proportions, and  
 89 (2) the Spearman correlation coefficient for each country, computed between population changes  
 90 and urban density values across individual Facebook tiles (Fig. 1). These indicators were then  
 91 examined in relation to socioeconomic characteristics to identify potential underlying drivers of  
 92 country-level differences.



93

94 **Fig. 1 The analytical framework for quantifying patterns of population redistribution.** Colour  
 95 transitions from green to grey represent a gradient from very low to very high urban density.  
 96 Facebook data (tile level) were overlaid with the “built-up area” class from the Esri 2020 Land Cover  
 97 dataset to characterise population changes across the urban density gradient within each country.  
 98 Two country-level indicators (Indicators 1 and 2) were calculated based on tile-level data for each  
 99 country (see Methods), to quantify shifts between urban and rural areas and changes along the  
 100 urban density gradient, respectively. This figure was created using resources from Flaticon.com, with  
 101 specific author attributions provided in the Acknowledgments.

102

### 103 Changes in urban-rural population distribution

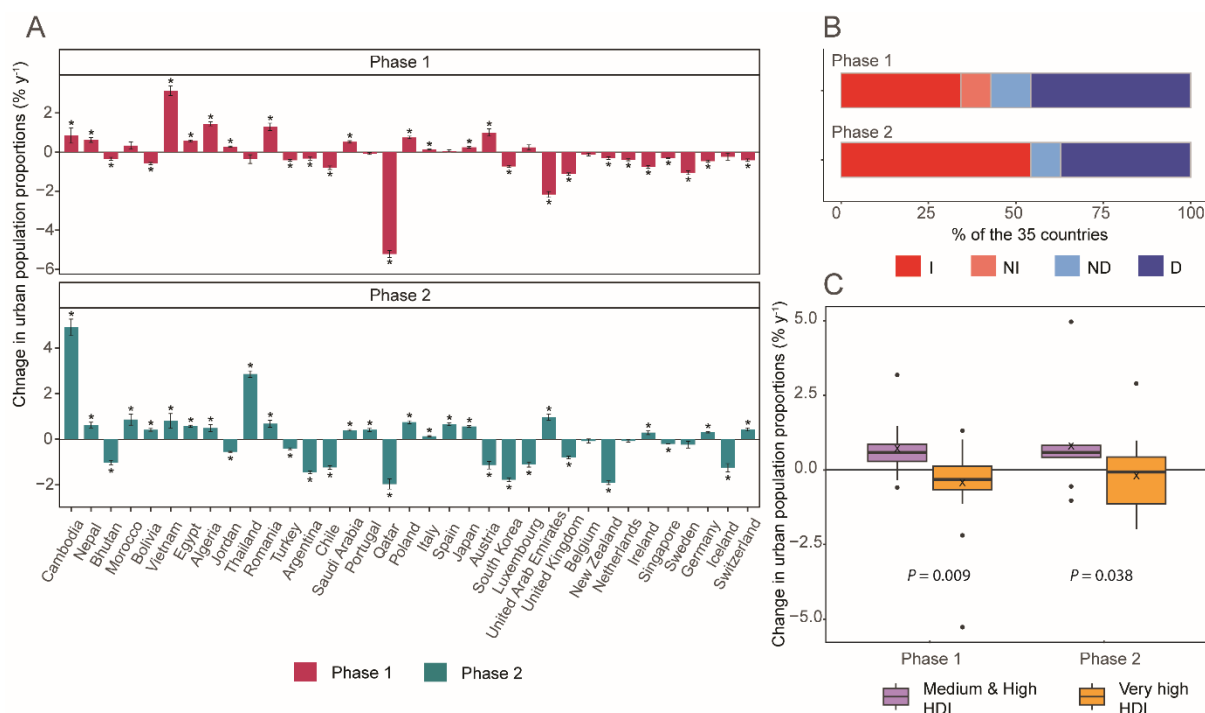
104 Given the varying impact of COVID-19 on population dynamics across countries during the study  
 105 period (March/April/May 2020 to May 2022; see Supplementary Table 5), we applied a data-driven  
 106 structural breakpoint analysis to weekly urban population proportion data (See Methods;  
 107 Supplementary Fig. 4). This automatically identified a single significant breakpoint for most countries,  
 108 allowing us to define two phases: Phase 1 (early response phase) and Phase 2 (later response phase).  
 109 The approach reflects actual changes in population distribution in responses to the pandemic and  
 110 associated restrictions, informed by previous work indicating that major shifts often correspond with  
 111 critical pandemic response stages<sup>20</sup>, and accounts for the fact that even identical restrictions may  
 112 have had different effect and levels of public compliance across pandemic waves and countries<sup>34,35</sup>.

113 Urban areas were defined as regions with urban density exceeding 25%, while areas below this  
 114 threshold were classified as rural, based on a commonly used definition from the perspective of  
 115 physical urban land<sup>37,38</sup>. Sensitivity tests with alternative cutoffs (20%, 30%, 40% and 50%) were used  
 116 to estimate breakpoints and the direction and extent of changes in urban population proportions.  
 117 These tests showed no statistically significant differences compared to the 25% threshold ( $P > 0.5$ ;  
 118 see Supplementary Fig. 5), confirming the robustness of our classification.

119 Our findings revealed notable cross-country variations in urban population changes over time  
 120 (Indicator 1; Figs 1 and 2A). While over 70% of countries maintained consistent trend directions  
 121 across both phases, differences in magnitude were evident. Specifically, 13 out of 35 countries  
 122 (37.1%) experienced declining trends in urban population proportions in both phases, with six (New  
 123 Zealand, South Korea, Argentina, Iceland, Chile and Bhutan) showing greater declines in Phase 2.  
 124 Conversely, 12 countries experienced increasing trends throughout both phases, with four  
 125 (Cambodia, Morocco, Spain, Japan) showing larger increases in the later phase. Additionally, 10  
 126 countries exhibited contrasting trend directions between the two phases, indicating that the choice  
 127 of living in urban or rural areas for many of their population was impacted by the COVID-19  
 128 pandemic. Overall, more countries demonstrated a decreasing trend in Phase 1 (Fig. 2B).

129 When comparing urban population proportion changes between countries grouped by Human  
 130 Development Index (HDI), clear disparities emerged. Countries with very high HDI ( $\geq 0.8$ ) showed a  
 131 negative mean change, with a smaller decrease in Phase 2 (-0.199%/year) compared to Phase 1 (-  
 132 0.423%/year). In contrast, countries in middle & high HDI group ( $< 0.8$ ) displayed positive mean  
 133 changes, increasing slightly from Phase 1 (0.702%/year) to Phase 2 (0.790%/year) (Fig. 2C).

134



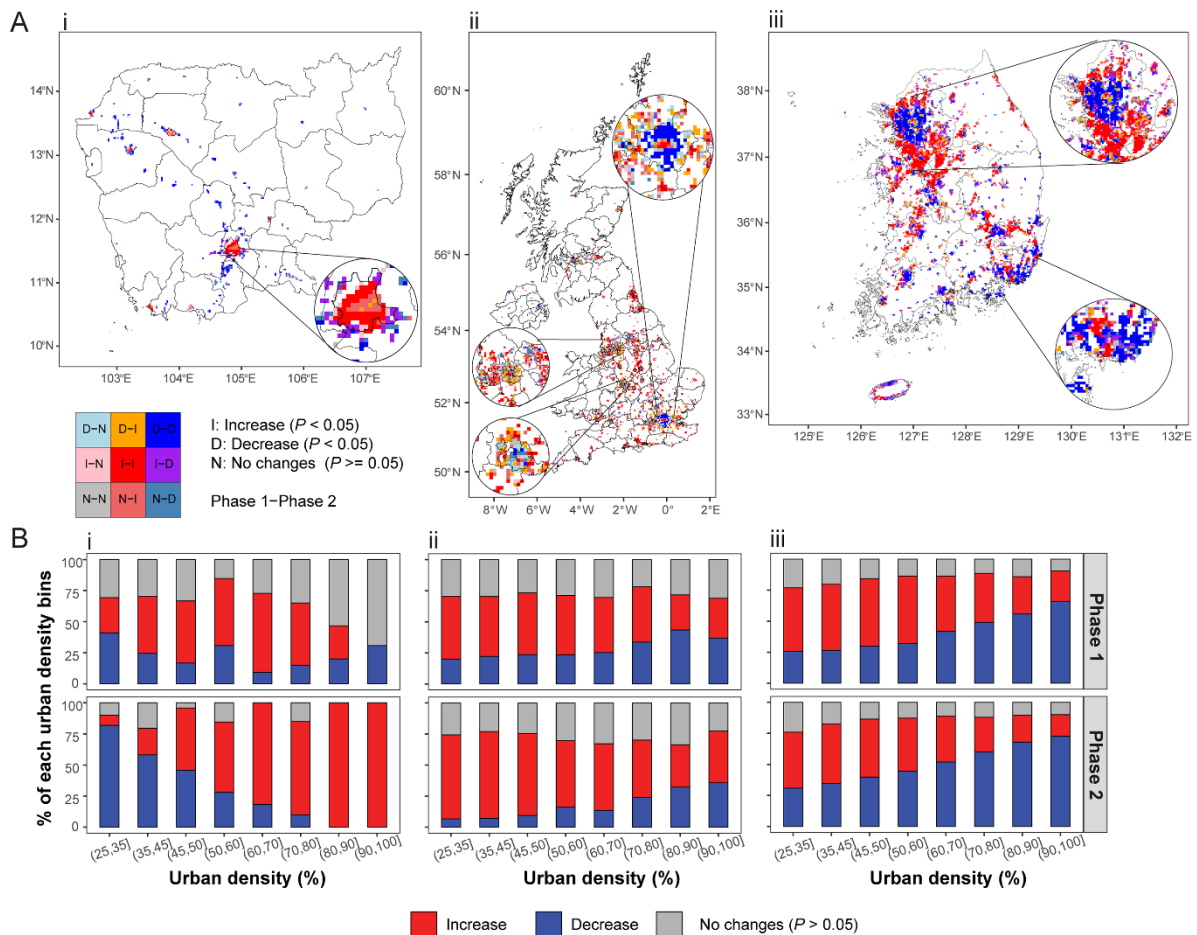
135  
 136 **Fig. 2 Contrasting patterns of change in urban population proportions across countries (Indicator**  
 137 **1).** (A) Changes in urban population proportions, estimated using robust linear regression on weekly  
 138 proportion data. Error bars represent standard errors of the regression estimates, and asterisks (\*)  
 139 denote statistical significance level ( $P < 0.05$ ). Significance was assessed using the two-sided robust F-  
 140 test with the “sfsmisc” package in R<sup>39</sup>. (B) Share of countries by change category: I for significant

141 increase, NI for non-significant increase, ND for non-significant decrease, and D for significant  
 142 decrease ( $P < 0.05$ ). (C) Box plots of changes between countries with middle & high ( $< 0.8$ ;  $n = 10$ )  
 143 and very high ( $\geq 0.8$ ;  $n = 25$ ) Human Development Index (HDI) levels. Boxes show the 25th to 75th  
 144 percentiles, with the median as a central line and the mean marked by "X." Whiskers extend 1.5  
 145 times the interquartile range. Significant differences between groups were tested using the two-  
 146 sided Wilcoxon test.

147

### 148 Change in population density along the urban density gradient

149 To further examine the nuances of population shifts, we assessed changes in population density at  
 150 the Facebook tile level within each country (see Methods). Our analysis revealed distinct spatial  
 151 patterns for each country (Fig. 3, see additional country plots in Supplementary Figs. 6 and 7).  
 152 Although urban core trends varied between countries, peripheral areas often exhibited shifted in the  
 153 opposite direction relative to their cores. For instance, during Phase 2, Cambodia showed population  
 154 growth in urban cores and declines in surrounding areas, whereas the UK and South Korea  
 155 experienced population losses in urban cores and growth in the periphery.



156

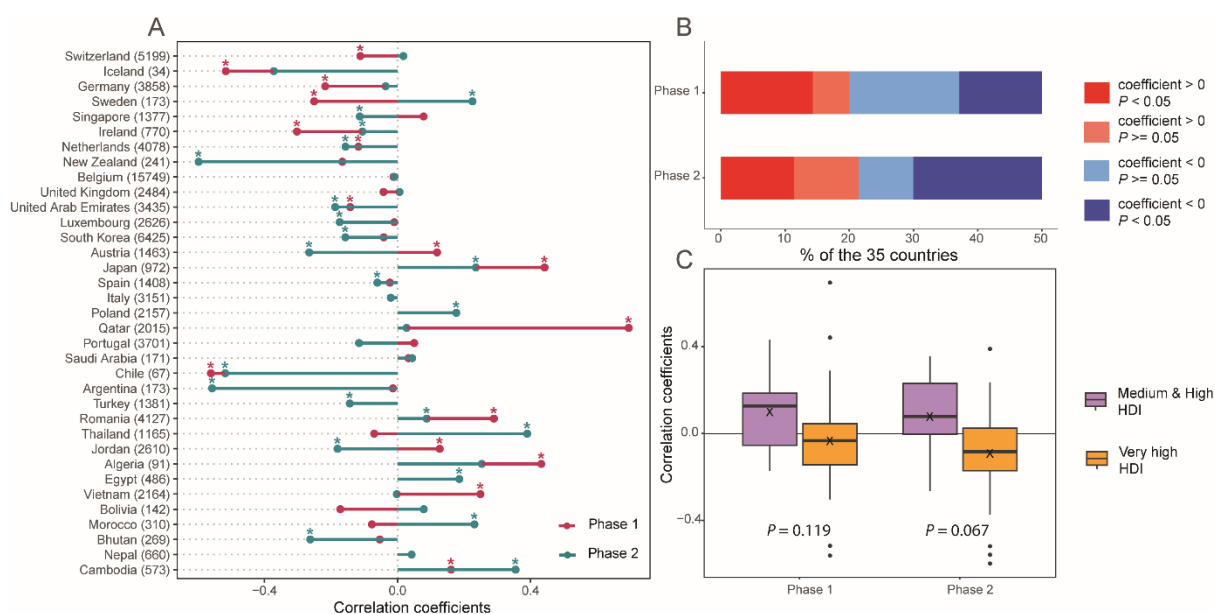
157 **Fig. 3 Spatial patterns of population density changes across urban density gradient within urban**  
 158 **areas. (A) Maps of population density change categories in urban Facebook tiles during two phases**  
 159 **for two example countries: (i) Cambodia, (ii) the United Kingdom and (iii) South Korea. See additional**  
 160 **country maps in Supplementary Fig. 6. Phase segmentation for each country has shown in**  
 161 **Supplementary Fig. 4. (B) Share of population density change categories along urban density bins.**

162 Bins were set at 5% increments for the lower 50% urban density and 10% increments beyond 50%,  
 163 accounting for the uneven distribution of urban density, as a greater number of tiles have lower  
 164 densities. See additional country plots in Supplementary Fig. 7. Country and administrative  
 165 boundaries were sourced from the Global Administrative Areas (GADM) spatial database (version  
 166 4.1).

167

168 To quantitatively summarise each country's trend of deconcentration or concentration along urban  
 169 density gradient, we calculated Spearman correlations by comparing population changes with urban  
 170 density values across individual Facebook tiles (Indicator 2; Figs. 1 and 4A). A modified t-test was  
 171 applied to evaluate the statistical significance of the correlations<sup>40</sup>, accounting for significant spatial  
 172 autocorrelation detected in all 35 countries (See Supplementary Table 6). A greater number of  
 173 countries showed significantly negative correlations in Phase 2 (Fig. 4B). However, no significant  
 174 differences in correlation coefficients were observed between the very high HDI and middle & high  
 175 HDI groups in either phase ( $P > 0.05$ ; Fig. 4C). While the mean correlation coefficient was negative in  
 176 the very high HDI countries, suggesting greater population dispersion, it remained positive in the  
 177 medium & high HDI groups, reflecting continued urban centre concentration in those regions.

178



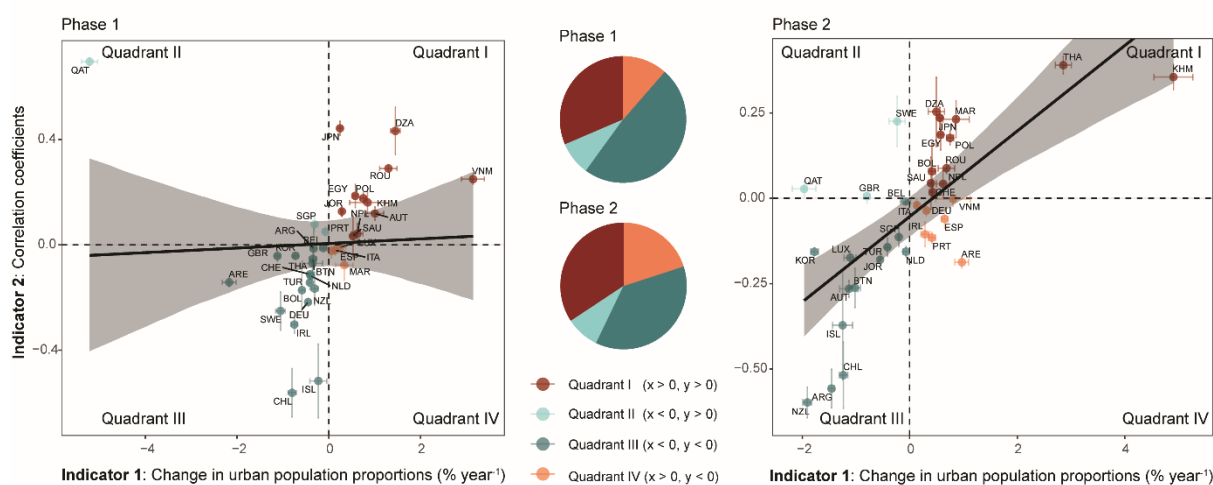
179

180 **Fig. 4 Correlation between population density changes and urban density (Indicator 2).** (A)  
 181 Spearman correlation coefficients; statistical significances were assessed using the modified t-test  
 182 ( $*P < 0.05$ ). The numbers in brackets indicate the number of urban area tiles used in the calculation.  
 183 (B) Share of countries by correlation category. (C) Box plots of correlation coefficients for countries  
 184 with middle & high ( $< 0.8$ ;  $n = 10$ ) and very high ( $\geq 0.8$ ;  $n = 25$ ) HDI levels. Boxes show the 25th to  
 185 75th percentiles, with the median as a central line and the mean marked by "X." Whiskers extend 1.5  
 186 times the interquartile range. Significant differences between groups were tested using the two-  
 187 sided Wilcoxon test.

188

189 **Country-level population redistribution patterns and associated socioeconomic**  
 190 **characteristics**

191 By combining the two indicators of changes in urban population proportions and correlation  
 192 coefficients between population density change and urban density, we identified distinct country-  
 193 level population redistribution patterns (Fig. 5). For example, in Phase 2, Spain (ESP in Quadrant IV)  
 194 showed an increase in urban population proportion but a negative correlation between population  
 195 changes and the urban density. This indicates that population shifts in Spain were not strictly an  
 196 urban-rural phenomenon but rather complex dynamics – a movement from both highly urbanised  
 197 and rural areas into moderately dense areas. While these two indicators were uncorrelated in Phase  
 198 1 (regression slope = 0.01; 95% credible interval (CrI): -0.06 to 0.08), a significant positive correlation  
 199 emerged in Phase 2 (regression slope = 0.13; 95% CrI: 0.08 to 0.17). This suggests that, in Phase 2,  
 200 countries experiencing higher increases in urban population proportion also tended to have  
 201 increased population concentrations in very high-density urban areas.

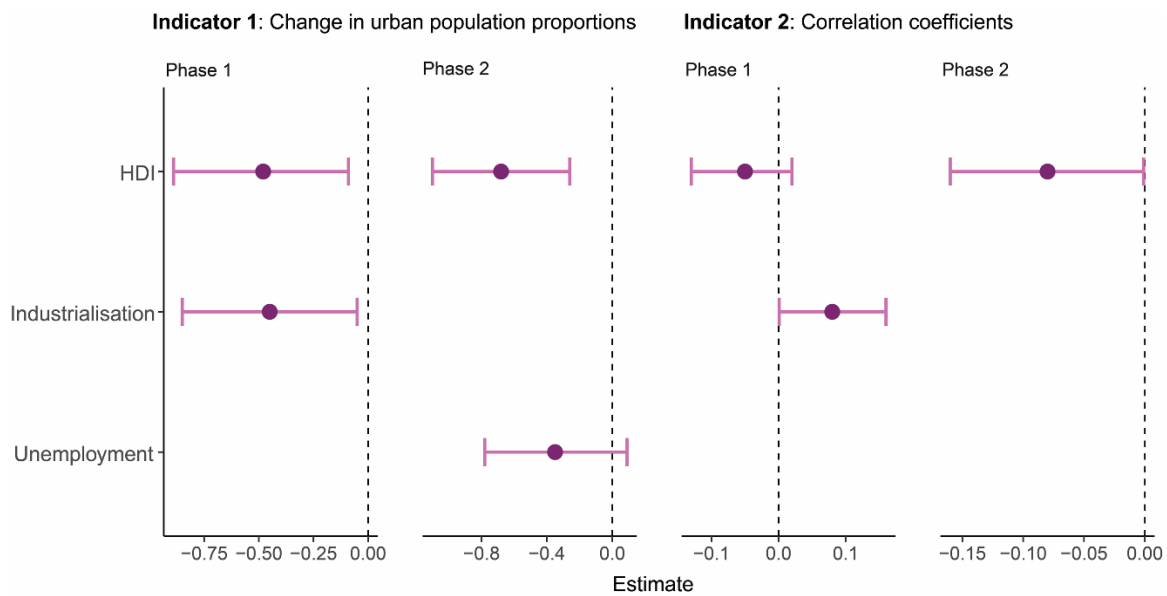


202 **Fig. 5 Two-indicator summary of country-level population redistribution patterns.** The x-axis  
 203 represents the annual changes in urban population proportions (Indicator 1), while the y-axis shows  
 204 the Spearman correlation coefficients between population density change and urban density  
 205 (Indicator 2). The relationship between these two dimensions of urban population changes across 35  
 206 countries was fitted using a Bayesian linear model (black fitted line with a 95% credible interval). Pie  
 207 charts in the centre display the proportion of countries in each quadrant for phase 1 (top) and phase  
 208 2 (bottom). Each country is marked using Country Codes Alpha-3 with the “countrycode” package in  
 209 R<sup>41</sup>.

211  
 212 The role of socioeconomic characteristics in shaping these redistribution patterns was further  
 213 explored through Bayesian multivariate linear modelling (see Methods). Country-level heterogeneity  
 214 in population redistribution patterns was negatively associated with HDI across both indicators and  
 215 phases, except for correlation coefficients (Indicator 2) in Phase 1. Countries with higher HDI  
 216 exhibited greater declines in urban population proportions (Phase 1: mean -0.48, 95% CrI -0.88 to -  
 217 0.09; Phase 2: -0.68, 95% CrI -1.11 to -0.28) and more negative correlation coefficients (Phase 1:  
 218 mean -0.05, 95% CrI -0.13 to 0.03; Phase 2: -0.15, 95% CrI -0.15 to -0.01) (Fig. 6). We also found  
 219 statistical evidence of a negative effect of industrialisation on urban population proportions  
 220 (Indicator 1: -0.45, 95% CrI -0.85 to -0.05) and a contrasting positive effect on correlation coefficients  
 221 (Indicator 2: 0.08, 95% CrI 0.00 to 0.16) in Phase 1.

222 When compared these effects with results from competing models (Supplementary Fig. 8), we found  
 223 similar patterns, although in some cases HDI showed strong evidence of negative association with  
 224 correlation coefficients in Phase 1. In contrast, no credible associations were found between  
 225 redistribution patterns and unemployment, income equality or the COVID-19 stringency index at the  
 226 country level, indicating that other structural factors might play a more dominant role in shaping  
 227 migration trends. A supplementary analysis of predictors excluded due to high correlation with HDI  
 228 (Supplementary Fig. 9) found strong statistical support for a negative effect of government  
 229 effectiveness and a positive effect of share of agriculture, forestry and fishing on changes in urban  
 230 population proportions (Supplementary Fig. 10), while individualism showed no credible evidence of  
 231 a negative effect.

232



233

234 **Fig. 6 Effects of socioeconomic characteristics on country-level population redistribution patterns.**  
 235 Indicator 1 is the change in urban population proportions (Phase 1:  $N = 35$ ,  $R^2 = 0.25$ ; Phase 2:  $N = 35$ ,  
 236  $R^2 = 0.27$ ). Indicator 2 is the Spearman correlation coefficients between population change and the  
 237 urban density gradient (Phase 1:  $N = 35$ ,  $R^2 = 0.19$ ; Phase 2:  $N = 35$ ,  $R^2 = 0.13$ ). The mean posterior  
 238 estimates of model parameters, with whiskers representing the 95% credible intervals for two  
 239 indicators and phases were derived from Bayesian linear models. See Supplementary Table 9 for  
 240 detailed posterior summaries for each variable.

241

## 242 Discussion

243 Our findings reveal broad yet heterogenous cross-country patterns of urban population  
 244 redistributions in response to COVID-19, aligning with earlier reports of an “urban exodus” during  
 245 the pandemic<sup>27,42,43</sup>. In the early stages of the pandemic, many countries experienced shifts toward  
 246 rural or lower-density urban areas, as restrictions, health concerns, and lifestyle changes disrupted  
 247 conventional patterns of urban living. Highly developed countries exhibited stronger trends toward  
 248 urban depopulation and spatial deconcentration, while middle- and high-HDI countries largely  
 249 continued along trajectories of urban population growth. However, some of these urban-rural shifts  
 250 appear to have been temporary. In the later phase of the pandemic, a partial reversal of earlier  
 251 trends was observed in several countries. Notably, countries that experienced larger increases in the

252 proportion of urban populations also tended to show greater growth in highly urbanised areas,  
253 consistent with the view that rapid urbanisation is driven by the availability of more and better-  
254 paying jobs concentrated in urban cores<sup>44</sup>. In contrast, no such relationship was observed in the  
255 early phase, when migration patterns were more heavily impacted by the pandemic and its  
256 associated disruptions.

257 A notable result of this study is that the two indicators we used (urban population proportions and  
258 correlations between population change and urban density) are associated with similar country-level  
259 socioeconomic characteristics, though not always in the same way across the two phases. The  
260 heterogeneity in population redistribution patterns across countries is negatively associated with  
261 HDI, aligning with previous observations in the Global North<sup>4,45</sup>, which is typically features high living  
262 conditions and advanced education. This suggests that in more developed contexts, where health,  
263 education, and income are relatively high, even less urbanised areas can offer a high quality of life.  
264 Improvements in overall development provide better access to essential services and more natural  
265 environments<sup>3</sup> outside urban cores, reducing the need to live in densely urbanised areas<sup>46</sup>. This  
266 relationship is also consistent with findings from the IMAGE database, which show strong migration  
267 from low- to high-density areas in low-HDI countries, while very high-HDI countries tend to exhibit  
268 flatter or reversed trends<sup>47</sup>. The negative effect of industrialisation on urban population proportions  
269 in phase 1 may reflect disruptions to industrial sectors during the early pandemic, which prompted  
270 people to return to rural areas amid economic uncertainty and in search of family support. Similar  
271 patterns have been observed during past crises, where individuals moved away from cities as a  
272 survival strategy<sup>48,49</sup>. However, in phase 2, this effect turned positive, although not statistically  
273 credible, likely reflecting the diminished impact of the pandemic. A similar general positive effect of  
274 the industrialisation<sup>51</sup> on the correlations between population change and urban density further  
275 indicates that the pull of urban cores within metropolitan areas persisted even during the pandemic,  
276 aligning with the well-recognised notion that industrialisation enhances the attractiveness of cities  
277 and promotes urbanisation<sup>50</sup>. In addition, countries with higher government effectiveness or a lower  
278 share of agriculture, forestry and fishing showed credible decreases in urban population proportions.  
279 This suggests that high-quality public services and policy implementation improve rural liveability  
280 and appeal to potential migrants<sup>52</sup>, while rural populations in agrarian economies remained  
281 attracted to urban areas, consistent with the rapid urban population growth observed in low-  
282 urbanisation countries that still rely on rural-based agricultural economies<sup>53,54</sup>. While we  
283 acknowledge that our analysis cannot capture all contributing factors, given the complexity of  
284 population redistribution and the constraints of global data availability, these findings nonetheless  
285 offer important implications for future planning.

286 Although it remains uncertain whether these trends will persist in the long term, the observed  
287 redistributions may signal future trajectories and highlight the importance of adapting future  
288 planning strategies tailored to countries' development levels. In very high-HDI countries, where the  
289 consistent depopulation in urban cores is accompanied by shifts to suburban or rural areas, short-  
290 term priorities include upgrading infrastructure in low-density areas to accommodate emerging  
291 demands<sup>6</sup>, such as expanding broadband access to support remote work and improving transport  
292 connectivity. Long-term challenges include managing growth in recipient rural areas to prevent  
293 uncontrolled sprawl. At the same time, strategic planning is necessary for those remaining in cities,  
294 where rising inequality and poverty are growing concerns<sup>6,16</sup>. This includes maintaining and  
295 repurposing underutilised infrastructure in depopulating high-density areas, such as water and  
296 electricity systems<sup>6,16</sup>, protecting low-income households from potentially rising service costs, and  
297 converting vacant land into green spaces to preserve urban liveability<sup>55</sup>. In contrast, middle- and  
298 high-HDI countries experiencing continued urbanisation should prioritise managing urban growth

299 while preventing rural decline. This includes developing industries that support remote work to  
300 alleviate urban pressure and investing in rural infrastructure to enhance its attractiveness. However,  
301 as these countries continue to develop, long-term planning should also anticipate potential shifts  
302 from high- to low-density areas. Additionally, in agriculturally dominant economies, the observed  
303 rural-to-urban migration raises concerns about a potential long-term risk to food security,  
304 highlighting the need for governments to invest in rural development and agricultural technology to  
305 sustain a stable farming workforce.

306 Shifting patterns of population distribution bring both possibilities and challenges for environmental  
307 sustainability<sup>13</sup>. While there are concerns about extensive development and occupation of local  
308 natural habitats by incoming residents<sup>56</sup>, evidence suggests that the environmental impact of this  
309 trend is complex and may not directly alter land use<sup>13</sup>. Migrants drawn to rural areas by the pursuit  
310 of better natural amenities often aim to protect and restore the landscapes, preserving the unique  
311 rural appeal that attracted them<sup>13,57</sup>. Meanwhile, the need to reshape idle infrastructure in  
312 depopulated cities poses challenges for urban sustainability and environmental equality for those  
313 remaining in high-density areas. Additionally, the shift from high- to low-density living raises  
314 concerns about increased energy consumption and its impact on environmental sustainability<sup>6</sup>. The  
315 exact environmental consequences of these changes require further exploration.

316 This analysis could also benefit resource allocation during future crises. Our finding that highly  
317 industrialised countries were most prone to a temporary urban exodus provides an important insight  
318 for preparedness<sup>48</sup>. Governments should anticipate that during a similar crisis, rural or low-density  
319 areas may experience temporary population increases. Crisis response strategies should therefore  
320 include increased allocation of medical supplies and essential goods to these regions<sup>58</sup>, along with  
321 strengthened support for local services to manage the additional strain caused by a temporary influx  
322 of people.

323 However, these findings were identified from a limited sample of 35 countries, primarily from  
324 Europe, Aisa, and South America. Several major countries such as the United States, China, and India,  
325 as well as low-income countries were not included due to data unavailability or low Facebook  
326 penetration. While these exclusions were necessary to ensure data quality and reliability, they  
327 inevitably constrain the global generalisability of our findings. Therefore, our results should be  
328 interpreted with caution, as they reflect trends and patterns across countries with relatively high  
329 mobile and Facebook usage, and it remains unclear if these patterns extend more broadly.  
330 Nevertheless, this cross-national analysis provides valuable insights into broader dynamics across  
331 diverse contexts. Future research should explore complementary data sources to fill gaps in  
332 underrepresented regions.

333 A key methodological decision in this study was to define COVID-19 response phases using a data-  
334 driven approach based on population dynamics rather than relying on official policy timelines. This  
335 choice was based on extensive evidence of behavioural fatigue<sup>35,59</sup>, where public adherence to  
336 interventions declines over time, causing a misalignment between government policies and actual  
337 population behaviour. For example, in the United States, early restrictions had a greater effect on  
338 social distancing than later interventions<sup>60</sup>, and similar patterns have been observed in mobility  
339 behaviours across different COVID-19 waves<sup>35,61</sup>. Despite this, we found that the COVID-19  
340 stringency index<sup>36</sup> generally declined or stabilised at a lower level following the identified breakpoint  
341 (Supplementary Fig. 11), and that differences between phases were statistically significant ( $P < 0.05$ )  
342 in most countries, except for Cambodia and those without identified breakpoints (Supplementary  
343 Fig. 12). We acknowledge that our period segmentation based on the dominant breakpoint may not  
344 fully capture temporal pattern in certain country (Supplementary Fig. 13). However, the consistent

345 framework was essential for our primary objective of comparing population redistribution across  
346 countries.

347 Another major limitation of this study is that the Facebook population data include only users who  
348 have enabled location services, which may not accurately represent the overall population dynamics.  
349 Indeed, data for each country may be influenced by the penetration of smart mobile devices,  
350 Facebook app usage, and the use of location services<sup>21,22</sup>. To mitigate bias, we selected countries  
351 where Facebook app coverage exceeded 40%<sup>62</sup>. However, since location services must be enabled on  
352 their devices, representativeness may be lower. Due to privacy protection constraints, no further  
353 user profiling information was available. Nevertheless, these data can reasonably represent  
354 population change trends<sup>30</sup> and capture migration patterns, as Facebook users typically belong to  
355 groups with high mobility<sup>27</sup>, especially since our study focuses on those who lived in high-density  
356 areas before moving away. To assess the spatial reliability of our dataset, we correlated the tile-level  
357 Facebook baseline count (mean over 90 days before the study period) with the widely used gridded  
358 population dataset GHS-POP 2020<sup>63</sup>, both representing populations before the COVID-19 pandemic.  
359 Across countries, correlations ranged from 0.61 (Bhutan) to 0.98 (Portugal and Argentina), with over  
360 94% exceeding 0.80 (Supplementary Fig. 2). Furthermore, using the United Kingdom as an example,  
361 we validated our estimates against 2021 Census data. Wider comparisons are challenging due to a  
362 lack of relevant census data during the pandemic; indeed, this lack of available data across countries  
363 is the reason we use Facebook data in this study. We found a high correlation of 0.97 between  
364 Facebook- and census-derived<sup>64</sup> population densities (Supplementary Fig. 15), as well as a moderate  
365 positive correlation of 0.55 between Facebook population trend and net migration from census  
366 origin-destination migration flows<sup>65</sup> (Supplementary Fig. 16) for England and Wales. The  
367 underestimation of change in the Facebook population is expected, as not all individuals use the  
368 platform or consent to data sharing. Together, these results validate the ability of our analysis to  
369 capture both real-world spatial patterns and migration trends. Other research using Facebook data in  
370 specific countries further support its reliability. Studies from the United Kingdom<sup>26</sup> and the United  
371 States<sup>66</sup> found Facebook data correlated well with census data, with no strong biases in age, ethnicity  
372 or race distributions. In Italy, although individuals aged 54 and above were underrepresented, this  
373 did not introduce spatial bias, as the territorial demographic distribution of age groups was relatively  
374 homogeneous<sup>29</sup>. In the Philippines, while younger age groups (18–34) were overrepresented, the  
375 observed population change trends remained reliable, as this demographic typically exhibits higher  
376 mobility<sup>30</sup>. Moreover, the usage of these social media data in government reports<sup>22</sup> during the  
377 COVID-19 pandemic further proved the value of the results derived from them.

378 Moreover, changes in Facebook usage throughout the study period may have influenced the results.  
379 People confined to their homes during lockdowns led to greater use of social media<sup>22</sup>. Although we  
380 eliminated changes from the collected data by normalising the population numbers, the possible  
381 uneven changes across different areas over time might skew the results. However, there is no  
382 evidence that Facebook usage trends varied spatially. Similarly, a study on mobile location data from  
383 SafeGraph in the United States showed that the relative sampling rate across geographic levels  
384 appeared relatively stable from 2020 to 2022<sup>67</sup>.

385 Despite inherent uncertainties in the data and the limitations of the analyses outlined above, the  
386 findings and insights from our study, based on a novel location dataset, provide a new cross-national  
387 perspective on population change patterns on various urban density in response to the shock of  
388 COVID-19. Our research helps identify countries that have experienced or are more likely to  
389 experience population redistribution out of highly urbanised areas, and highlights the importance of

390 adaptable rural-urban planning and policy frameworks that account for shifting population dynamics  
391 to address future challenges to societal and environmental sustainability.

392

## 393 **Methods**

### 394 **Facebook population data at tile level**

395 Facebook population data were aggregated spatially to Bing tile levels<sup>68</sup> by Meta across 8-hour  
396 periods during the COVID-19 pandemic. The spatial tile level and time period varied for different  
397 countries (see Supplementary Table 5), adapting to ensure computation updates within an 8-hour  
398 window and compliance with privacy standards. In general, our samples ranged from tile level 12  
399 (approximately 9.8 km at the equator) to tile level 16 (approximately 600 m at the equator). Time  
400 periods also varied by country and began in March, April, or May of 2020 and extended to the 21<sup>st</sup> or  
401 22<sup>nd</sup> of May 2022. For each 8-hour period (00:00–07:59, 08:00–15:59, 16:00–23:59 Coordinated  
402 Universal Time), the number of individual devices in each tile was collected. These devices  
403 correspond with a Facebook app user who has consented to share their mobile device location  
404 history with Meta. Locations are estimated using signals like Wi-Fi and mobile networks, GPS and  
405 sensor information where available. If a user appeared in different tiles during one time window,  
406 their location was assigned to the tile where they appeared most frequently. These data come with  
407 an associated baseline count, which is defined as the average number of users for at least 90 days  
408 before the start of data collection in each country<sup>21</sup>. Additionally, Meta applied privacy protection  
409 techniques, excluding any population or baseline lower than ten people for a specific time and date  
410 to ensure that the locations of individuals or small groups cannot be identified<sup>21</sup>. To avoid bias  
411 caused by excluded values in rural areas, we applied a two-step imputation procedure, as described  
412 in ref.<sup>20</sup>, to estimate missing data for specific dates. First, the baseline count for a tile with missing  
413 data was estimated either from valid observations on other dates or, when unavailable, from a linear  
414 regression between Facebook baseline counts and WorldPop 2019 population data<sup>69</sup> within each  
415 country. Second, missing value was reconstructed using the imputed baseline together with its  
416 corresponding percent change from baseline reported by Facebook for that date. Further imputation  
417 details are provided in ref.<sup>20</sup> and, for convenience, in Supplementary Note 1.

418 We then analysed the population changes during the night-time window on workdays in each  
419 country to explore residential redistribution, considering that people are likely to be at home during  
420 that time. The workdays are not identical across the globe; specific workdays for each country can be  
421 found in Supplementary Table 5. We excluded the half-working day, such as Friday in the United Arab  
422 Emirates, to more accurately capture their normal living location. We used the aggregated weekly  
423 averages of daily populations on workdays to capture the main residence and reduce the effect of  
424 occasional overnight/late night trips on our results. Additionally, the procedure to eliminate the  
425 seasonal variation based on weekly observations (see the details below) and the use of robust linear  
426 regression for trend estimation (see below) also helped reduce the impact of variations during  
427 holiday periods.

428 Moreover, the total population counts collected showed an overall trend and daily fluctuations due  
429 to limitations in internet access and active user availability<sup>21,22</sup>. To address this, we normalised the  
430 counts to eliminate changes caused by data collection<sup>20</sup>, assuming that the representativeness of  
431 Facebook data for each tile remained constant throughout the period. Specifically, we adjusted the  
432 counts for each tile on a given date by first calculating each tile's share of the total daily population  
433 across all tiles, and then scaled these proportions by the median of the daily total population

434 observed throughout the study period <sup>20</sup>. Thus, these adjusted numbers represent the population  
435 redistribution <sup>70</sup>, control for changes in Facebook usage, and are used to infer distribution patterns  
436 across different urban density areas.

437

#### 438 **Study areas**

439 A total of 35 countries were selected based on the following criteria related to data availability and  
440 quality: 1) the availability of Facebook population data at the tile level from Meta <sup>21</sup>; 2) Facebook  
441 data covering more than two years to allow for the detection and removal of seasonal variations; 3)  
442 data with a spatial resolution at Bing tile level 12 or higher (approximately  $\leq 9.8$  km at the  
443 equator)<sup>68</sup>, as too coarse spatial details cannot provide effective information; 4) an estimated high  
444 penetration of Facebook usage (over 40% of the total population) <sup>62</sup>, which will likely reduce  
445 potential bias in using Facebook data to infer population-level mobility. The 40% penetration  
446 threshold was selected to optimise the trade-off between high platform penetration and a sufficient  
447 sample size for cross-national analysis. At this level, only two countries were excluded compared to  
448 the 30% threshold (from 37 to 35), whereas increasing it to 50% would have resulted in a much  
449 larger loss of eight countries, reducing the sample to 27 (Supplementary Fig. 17). The final sample of  
450 35 countries contains 15.3% of the global population <sup>1</sup>, including 23 high-income countries and 12  
451 middle-income countries. Notably, these criteria resulted in the exclusion of low-income countries,  
452 which generally have low smartphone adoption rates <sup>71</sup> and very limited Facebook usage <sup>62</sup>. Several  
453 major countries such as the United States, China and India were also excluded due to data  
454 unavailability or low Facebook penetration. Furthermore, we conducted a sensitivity analysis using  
455 the 27 countries that met a stricter 50% penetration criterion to confirm the robustness of our  
456 predictor effects (Supplementary Fig. 18).

457

#### 458 **Urban density and urban-rural definitions**

459 We chose to use percentage cover of built-up areas at each country's spatial tiles to characterise  
460 their degrees of urbanisation. The Esri 2020 Land Cover dataset was selected due to its higher  
461 accuracy in built-up areas (95.8% user's accuracy and 83.7% producer's accuracy) compared to other  
462 land use and land cover datasets of 2020 <sup>72</sup>. This global map, derived from European Space Agency  
463 (ESA) Sentinel-2 imagery at 10m resolution, provides 9 classes of land cover. The class "built-up area"  
464 includes human made structures, major road and rail networks, and large homogenous impervious  
465 surfaces <sup>72</sup>.

466 In this study, urban areas are defined as areas with more than 25% built-up areas <sup>37</sup>, based on a  
467 commonly used definition from the perspective of physical urban land <sup>37,38</sup>. It is important to note  
468 that this classification reflects the degree of physical urban density for each tile, without considering  
469 their contiguity (neighbouring tiles).

470

#### 471 **Response phases segmentation and population change calculation**

472 To divide the study period into distinct of pandemic response, we identified abrupt changes in  
473 weekly urban population proportion data (2020–2022) for each country using the Breaks For Additive  
474 Seasonal and Trend (BFAST) algorithm <sup>73</sup>. This data-driven segmentation was conducted to account  
475 for the impacts of COVID-19 restrictions, recognising that identical restrictions might have different

476 effects across pandemic waves and countries<sup>34,35,74</sup>. BFAST was implemented using the “BFAST”  
477 package in R.

478 The BFAST algorithm first applied Seasonal-Trend decomposition using Loess (STL)<sup>75</sup> to eliminate the  
479 seasonal variation for our weekly Facebook population data<sup>20</sup>. STL is widely used in trend analysis  
480 because it is not sensitive to outliers, applicable to various seasonal data types, and computationally  
481 efficient<sup>76,77</sup>. Detailed STL procedures are described in Cleveland et al., (1990).

482 BFAST then tested for any abrupt changes in the deseasoned data using the Moving SUM (MOSUM)  
483 approach<sup>78</sup>. The sensitivity of breakpoint detection was controlled by the minimum interval setting.  
484 We selected this setting based on a sensitivity analysis that tested intervals ranging from 10% to 50%  
485 of the total study period for each country (Supplementary Fig. 13). An interval of 40% (approximately  
486 44 weeks) yielded the most stable and consistent results across countries (Supplementary Fig. 14)  
487 and was therefore used in this study. This interval also effectively captured dominant shifts while  
488 filtering out minor fluctuations. When a significant change was detected ( $P < 0.05$ ), the breakpoint  
489 was estimated by minimising the Bayesian Information Criterion (BIC)<sup>79</sup>. This involved an iterative  
490 procedure that minimised the residual sum of squares to estimate the optimal break positions and  
491 their 95% confidence intervals. In most countries in our analysis, BFAST identified one significant  
492 breakpoint, which we used to define two analytical phases: Phase 1 (early response) preceding the  
493 break; and Phase 2 (later response) following it.

494 Finally, changes were quantified using slopes and  $P$  values from robust linear regression fitted to the  
495 pre- and post-breakpoint segments. The robust linear regression, performed by “MASS” package in R,  
496 offers greater robustness to outliers, helping to mitigate the impact of unexpected events like  
497 holidays<sup>80</sup>.

498 To segment phases and analyse changes in urban-rural population redistributions, we calculated the  
499 weekly population proportion ( $Pro$ ) in urban areas,

$$500 \quad Pro = \sum_{i=1}^N (S_{n,i} \times X_i) / \sum_{i=1}^N (S_{n,i}) \quad (1)$$

501 where  $X_i = 1$  if the urban density of tile  $i$  is exceeding 25%, and  $X_i = 0$  otherwise.  $N$  is the total  
502 number of tiles for this country, and  $S_{n,i}$  is the Facebook population counts for tile  $i$ . Changes in  $Pro$   
503 (Indicator 1) summarised country-level changes in urban-rural population distributions.

504 To assess finer-scale changes in population density along the urban density gradient, we analysed  
505 tile-level population counts for tiles with adequate data coverage, that is, those with at least two  
506 complete periods required to identify seasonal components. We applied robust linear regression at  
507 each tile to estimate changes in population density within the phases defined by the breakpoint of its  
508 respective country. These were used to explore finer-scale dynamics along the urban density  
509 gradient. Spearman correlation coefficients between these changes and the corresponding urban  
510 density values (Indicator 2) were computed to summarise country-level patterns along the urban  
511 density gradient.

512

### 513 **Statistical analyses of country-level differences**

514 To explore the relationship between two indicators of country-level redistribution patterns, we fitted  
515 Bayesian linear models using the “brms” package in R<sup>81</sup>, with default non/weakly informative priors.  
516 The response variable was the Spearman correlation between population change and urban density

517 (Indicator 2), and the predictor was the change in urban population proportions (Indicator 1). Their  
518 standard errors (SEs) were estimated separately from the “vcmeta” package<sup>82</sup> and robust linear  
519 regression. Models for both response phases were run using four chains, each with 2000 iterations  
520 and 1000 warm-up iterations.

521 We also assessed the extent to which Indicator 1 and 2 were associated with country-level  
522 socioeconomic characteristics across the two response phases, using four additional Bayesian  
523 multivariate linear models<sup>83</sup>. Each indicator served as the response variable in separate models, with  
524 their SEs as measurement errors. Based on previous research, we selected eight potential  
525 explanatory variables spanning socioeconomic conditions, industrial structure, culture, governance,  
526 and COVID-19 interventions<sup>36</sup> (see Supplementary Table 7 for data sources). We included the Human  
527 Development Index (HDI)<sup>46</sup>, as most studies on urban-to-rural redistribution have primarily focused  
528 on countries in the Global North, which are typically characterised by higher levels of social and  
529 economic development. To capture aspects of inequality not reflected in the HDI<sup>84</sup>, we added  
530 income inequality<sup>85</sup>, a major component of urban–rural gap that can drive migration<sup>86</sup>. Industrial  
531 structure was measured using the share of industry value and the share of agriculture, forestry, and  
532 fishing value, to capture the degree of economic transformation, as shifts from agriculture- to  
533 industry- or services-led economies often increase urban pull factors<sup>50,87,88</sup>. We also included  
534 unemployment to account for economically motivated migration<sup>48,89</sup>; individualism<sup>90</sup>, as evidence  
535 links higher residential mobility to societies that prioritise individual autonomy over collective  
536 identity<sup>91,92</sup>; and government effectiveness, to capture the quality of public services and policy  
537 implementation that determine regional liveability and appeal to potential migrants<sup>52,93</sup>. Finally, to  
538 capture the impact of pandemic policy, we used the COVID-19 stringency index<sup>36</sup>, which reflects the  
539 severity of government-imposed restrictions likely to influence residential decisions. To account for  
540 multicollinearity of these variables, we calculated pair-wise Pearson correlations and the variance  
541 inflation factor (VIF) in linear regressions. We excluded variables with a correlation coefficient higher  
542 than 0.7 (individualism, government effectiveness and the share of agriculture, forestry value;  
543 Supplementary Fig. 9), with all retained variables had a VIF below 2.5. For completeness, we report a  
544 sensitivity analysis in the Supplementary Fig. 10 where each excluded variable was substituted into  
545 the model in place of its highly correlated counterpart. All predictors were standardised prior to  
546 modelling.

547 These models were run with four Markov chains, each with 2,000 iterations and 1,000 warm-up  
548 iterations, using default priors. Convergence on all four chains was achieved for each model (rhat =  
549 1.00 for all coefficient estimates). Given our limited sample size and to avoid overfitting, we selected  
550 the final models based on the lowest leave-one-out cross-validation information criterion (LOOIC;  
551 calculated using R package “loo”<sup>94</sup>) after assessing all possible predictor combinations. As a  
552 sensitivity analysis, we presented competing models with similarly low LOOIC scores in  
553 Supplementary Fig. 8 to confirm that the effects of key predictors were robust across different model  
554 specifications.

555

## 556 **Data availability**

557 The Facebook population data (tile level) for this study were obtained through Meta’s AI for Good  
558 program. They are not publicly available due to licensing agreements. Information on requesting  
559 access to this data can be found at <https://dataforgood.facebook.com/>. All other data used in this  
560 paper are publicly available, with sources listed in the text. These include the Esri 2020 Land Cover  
561 dataset (<https://livingatlas.arcgis.com/landcover/>), the Human Development Index

562 (<https://hdr.undp.org/data-center/human-development-index#/indicies/HDI>), income inequality  
563 data from the Standardized World Income Inequality Database v.9.8  
564 (<https://doi.org/10.7910/DVN/LM4OWF>), government effectiveness, unemployment, share of  
565 industry, share of agriculture, forestry, and fishing data from the World Bank  
566 (<https://data.worldbank.org/indicator>), Geert Hofstede's Individualism versus Collectivism scores  
567 (<https://geerthofstede.com/culture-geert-hofstede-gert-jan-hofstede/6d-model-of-national-culture/>), and COVID-19 stringency index from the Oxford Covid-19 Government Response Tracker  
568 (<https://www.bsg.ox.ac.uk/research/covid-19-government-response-tracker>). Country and  
569 administrative boundaries were sourced from the Global Administrative Areas spatial database  
570 (<https://gadm.org/data.html>).  
571

572

## 573 **Acknowledgments**

574 This work was supported by the ESRC South Coast Doctoral Training Partnership (grant number  
575 ES/P000673/1), as part of the first author's doctoral research, and the National Institute for Health  
576 (MIDAS Mobility R01AI160780) and the Horizon Europe (UKRI grant number 10041831). SL and AJT  
577 are supported by funding from the Bill & Melinda Gates Foundation (OPP1134076, INV-024911), the  
578 National Institutes of Health (R01AI160780), the Horizon Europe program (MOOD 874850) and the  
579 U.S. National Science Foundation (DMS-2327797). The authors would like to also acknowledge the AI  
580 for Good program at Meta for sharing data and thank Dr Tim O'Riordan, Dr Eimear Cleary, Dr Theo  
581 Chan, and Dr Fatumah Atuhaire for Facebook population data collection. We thank Yuxuan Guo, Dr  
582 Nick Dorward, Dr Rebecca Collins and Dr Sarchil Qader for discussions and suggestions that improved  
583 the manuscript. The icons used in Figure 1 were designed by Freepik, Nikita Golubev, mnauliady,  
584 kerismaker, Karyative, Prosymbols Premium, DinosoftLabs, juicy\_fish, Vectors Market, Dewi Sari, and  
585 Sudowoodo from [www.flaticon.com](http://www.flaticon.com).

586

587

## 588 **Author information**

589 Authors and Affiliations

590 **School of Geography and Environmental Science, University of Southampton, Southampton SO17**  
591 **1BJ, United Kingdom**

592 Qianwen Duan & Felix Eigenbrod

593

594 **WorldPop, School of Geography and Environmental Science, University of Southampton,**  
595 **Southampton SO17 1BJ, United Kingdom**

596 Shengjie Lai, Andrew J. Tatem & Jessica Steele

597

598 **Dipartimento di Scienze della Terra "Ardito Desio", Università degli Studi di Milano, Via Mangiagalli**  
599 **34, 20133 Milan, Italy**

600 Alessandro Sorichetta

601

602 Contributions

603 QD, SL, AS and FE contributed to conceptualisation. QD and FE designed the research. QD, SL and AJT  
604 contributed to Facebook data curation. QD conducted formal analysis, visualisation and wrote the  
605 manuscript. FE, SL and JS helped to improve the methodology. All authors commented on and  
606 revised drafts of the manuscript.

607  
608 Corresponding author  
609 Correspondence to Qianwen Duan  
610

611 **Ethics declarations**

612 The authors declare no competing interests.

613

614 **References**

- 615 1. World Bank. World Bank Open Data. (2022).
- 616 2. Wahba Tadros, S. N. *et al. Demographic Trends and Urbanization.*  
617 <http://documents.worldbank.org/curated/en/260581617988607640/Demographic-Trends-and->  
618 [Urbanization](http://documents.worldbank.org/curated/en/260581617988607640/Demographic-Trends-and-) (2021).
- 619 3. Halfacree, K. To revitalise counterurbanisation research? Recognising an international and fuller  
620 picture. *Population, Space and Place* **14**, 479–495 (2008).
- 621 4. Rowe, F., Bell, M., Bernard, A., Charles-Edwards, E. & Ueffing, P. Impact of internal migration on  
622 population redistribution in Europe: Urbanisation, counterurbanisation or spatial equilibrium?  
623 *CPoS* **44**, (2019).
- 624 5. Niva, V. *et al.* World’s human migration patterns in 2000–2019 unveiled by high-resolution data.  
625 *Nat Hum Behav* **7**, 2023–2037 (2023).
- 626 6. Sutradhar, U., Spearing, L. & Derrible, S. Depopulation and associated challenges for US cities by  
627 2100. *Nat Cities* **1**, 51–61 (2024).
- 628 7. Gamlen, A. Migration isn’t increasing, border restrictions don’t reduce crossings — and other  
629 home truths. *Nature* **623**, 683–684 (2023).
- 630 8. Wolff, M. & Mykhnenko, V. COVID-19 as a game-changer? The impact of the pandemic on urban  
631 trajectories. *Cities* **134**, 104162 (2023).
- 632 9. Stawarz, N., Rosenbaum-Feldbrügge, M., Sander, N., Sulak, H. & Knobloch, V. The impact of the  
633 COVID-19 pandemic on internal migration in Germany: A descriptive analysis. *Population, Space*  
634 *and Place* **28**, e2566 (2022).

- 635 10. Ilham, M. A., Fonzone, A., Fountas, G. & Mora, L. To move or not to move: A review of  
636 residential relocation trends after COVID-19. *Cities* **151**, 105078 (2024).
- 637 11. Güneralp, B., Reba, M., Hales, B. U., Wentz, E. A. & Seto, K. C. Trends in urban land expansion,  
638 density, and land transitions from 1970 to 2010: a global synthesis. *Environ. Res. Lett.* **15**,  
639 044015 (2020).
- 640 12. Cheng, L., Yang, M., De Vos, J. & Witlox, F. Examining geographical accessibility to multi-tier  
641 hospital care services for the elderly: A focus on spatial equity. *Journal of Transport & Health* **19**,  
642 100926 (2020).
- 643 13. Herrero-Jáuregui, C. & Concepción, E. D. Effects of counter-urbanization on Mediterranean rural  
644 landscapes. *Landsc Ecol* **38**, 3695–3711 (2023).
- 645 14. Huang, S. *et al.* Widespread global exacerbation of extreme drought induced by urbanization.  
646 *Nat Cities* **1**, 597–609 (2024).
- 647 15. Jimenez, Y. G. *et al.* Counterurbanization: A neglected pathway of forest transition. *Ambio* **51**,  
648 823–835 (2022).
- 649 16. Faust, K. M., Abraham, D. M. & DeLaurentis, D. Coupled Human and Water Infrastructure  
650 Systems Sector Interdependencies: Framework Evaluating the Impact of Cities Experiencing  
651 Urban Decline. *Journal of Water Resources Planning and Management* **143**, 04017043 (2017).
- 652 17. Leyk, S. *et al.* The spatial allocation of population: a review of large-scale gridded population  
653 data products and their fitness for use. *Earth System Science Data* **11**, 1385–1409 (2019).
- 654 18. Lai, S. *et al.* Assessing the Effect of Global Travel and Contact Restrictions on Mitigating the  
655 COVID-19 Pandemic. *Engineering (Beijing)* **7**, 914–923 (2021).
- 656 19. Cot, C., Cacciapaglia, G. & Sannino, F. Mining Google and Apple mobility data: temporal anatomy  
657 for COVID-19 social distancing. *Sci Rep* **11**, 4150 (2021).
- 658 20. Duan, Q. *et al.* Identifying counter-urbanisation using Facebook’s user count data. *Habitat*  
659 *International* **150**, 103113 (2024).

- 660 21. Maas, P. Facebook Disaster Maps: Aggregate Insights for Crisis Response & Recovery. in  
661 *Proceedings of the 25th ACM SIGKDD International Conference on Knowledge Discovery & Data*  
662 *Mining* 3173–3173 (ACM, Anchorage AK USA, 2019). doi:10.1145/3292500.3340412.
- 663 22. Shepherd, H. E. R., Atherden, F. S., Chan, H. M. T., Loveridge, A. & Tatem, A. J. Domestic and  
664 international mobility trends in the United Kingdom during the COVID-19 pandemic: an analysis  
665 of facebook data. *International Journal of Health Geographics* **20**, 46 (2021).
- 666 23. Jia, S., Kim, S. H., Nghiem, S. V., Doherty, P. & Kafatos, M. C. Patterns of population displacement  
667 during mega-fires in California detected using Facebook Disaster Maps. *Environ. Res. Lett.* **15**,  
668 074029 (2020).
- 669 24. Rashid, M. M., Tirtha, S. D., Eluru, N. & Hasan, S. Understanding hurricane evacuation behavior  
670 from Facebook data. *International Journal of Disaster Risk Reduction* **116**, 105147 (2025).
- 671 25. Jamal, T. B. & Hasan, S. Understanding the loss in community resilience due to hurricanes using  
672 Facebook Data. *International Journal of Disaster Risk Reduction* **97**, 104036 (2023).
- 673 26. Gibbs, H. *et al.* Detecting behavioural changes in human movement to inform the spatial scale of  
674 interventions against COVID-19. *PLOS Computational Biology* **17**, e1009162 (2021).
- 675 27. Rowe, F., Calafiore, A., Arribas-Bel, D., Samardzhiev, K. & Fleischmann, M. Urban exodus?  
676 Understanding human mobility in Britain during the COVID-19 pandemic using Meta-Facebook  
677 data. *Population, Space and Place* **29**, e2637 (2023).
- 678 28. Silva, L., Bezzo, F. B., Manfredini, F., Giavarini, V. & Di Rosa, C. Away from the cities? A medium-  
679 to-long-term investigation of how the COVID-19 pandemic has changed population spatial  
680 patterns in Italy. *European Urban and Regional Studies* **32**, 147–165 (2025).
- 681 29. Beria, P. & Lunkar, V. Presence and mobility of the population during the first wave of Covid-19  
682 outbreak and lockdown in Italy. *Sustainable Cities and Society* **65**, 102616 (2021).
- 683 30. Dujardin, S., Vibar, A. A. B., Paulus, R., Kienberger, S. & Linard, C. Dynamic Social Vulnerability  
684 Mapping Using Facebook Data. *Population, Space and Place* **31**, e70022 (2025).

- 685 31. Cabrera, C., Rowe, F., González-Leonardo, M., Nasuto, A. & Neville, R. Long-term disparities in  
686 the recovery of urban mobility after COVID-19 in Latin America. Preprint at  
687 <https://doi.org/10.48550/arXiv.2504.15871> (2025).
- 688 32. Zhou, Y. *et al.* Satellite mapping of urban built-up heights reveals extreme infrastructure gaps  
689 and inequalities in the Global South. *Proceedings of the National Academy of Sciences* **119**,  
690 e2214813119 (2022).
- 691 33. Xu, G. *et al.* Underlying rules of evolutionary urban systems in Africa. *Nat Cities* **2**, 327–335  
692 (2025).
- 693 34. Ge, Y. *et al.* Untangling the changing impact of non-pharmaceutical interventions and  
694 vaccination on European COVID-19 trajectories. *Nat Commun* **13**, 3106 (2022).
- 695 35. Kim, S., Jang, K. & Yeo, J. Non-linear impacts of COVID-19 pandemic on human mobility: Lessons  
696 from its variations across three pandemic waves. *Sustainable Cities and Society* **97**, 104769  
697 (2023).
- 698 36. Hale, T. *et al.* A global panel database of pandemic policies (Oxford COVID-19 Government  
699 Response Tracker). *Nat Hum Behav* **5**, 529–538 (2021).
- 700 37. Schneider, A., Friedl, M. A. & Potere, D. Mapping global urban areas using MODIS 500-m data:  
701 New methods and datasets based on ‘urban ecoregions’. *Remote Sensing of Environment* **114**,  
702 1733–1746 (2010).
- 703 38. Zhang, X. *et al.* A large but transient carbon sink from urbanization and rural depopulation in  
704 China. *Nat Sustain* **5**, 321–328 (2022).
- 705 39. Ghosh, T. S., Shanahan, F. & O’Toole, P. W. Toward an improved definition of a healthy  
706 microbiome for healthy aging. *Nat Aging* **2**, 1054–1069 (2022).
- 707 40. Dutilleul, P., Clifford, P., Richardson, S. & Hemon, D. Modifying the t Test for Assessing the  
708 Correlation Between Two Spatial Processes. *Biometrics* **49**, 305–314 (1993).
- 709 41. Arel-Bundock, V., Enevoldsen, N. & Yetman, C. countrycode: An R package to convert country  
710 names and country codes. *Journal of Open Source Software* **3**, 848 (2018).

- 711 42. Gkartzios, M. & Halfacree, K. Editorial. Counterurbanisation, again: Rural mobilities,  
712 representations, power and policies. *Habitat International* **140**, 102906 (2023).
- 713 43. Halfacree, K. Counterurbanisation in post-covid-19 times. Signifier of resurgent interest in rural  
714 space across the global North? *Journal of Rural Studies* **110**, 103378 (2024).
- 715 44. Lucas, R. E., Jr. Life earnings and rural-urban migration. *Journal of political economy* **112**, S29–  
716 S59 (2004).
- 717 45. Dilley, L., Gkartzios, M. & Odagiri, T. Developing counterurbanisation: Making sense of rural  
718 mobility and governance in Japan. *Habitat International* **125**, 102595 (2022).
- 719 46. United Nations Development Programme. *Human Development Report 2019: Beyond Income,*  
720 *beyond Averages, beyond Today: Inequalities in Human Development in the 21st Century.*  
721 <https://hdr.undp.org/system/files/documents/hdr2019.pdf> (2019).
- 722 47. Rees, P. *et al.* The Impact of Internal Migration on Population Redistribution: an International  
723 Comparison. *Population, Space and Place* **23**, e2036 (2017).
- 724 48. Gkartzios, M. ‘Leaving Athens’: Narratives of counterurbanisation in times of crisis. *Journal of*  
725 *Rural Studies* **32**, 158–167 (2013).
- 726 49. Anastasiou, E. & Duquenne, M.-N. Determinants and Spatial Patterns of Counterurbanization in  
727 Times of Crisis: Evidence from Greece. *Population Review* **59**, (2020).
- 728 50. Sun, Y., Jiao, L., Guo, Y. & Xu, Z. Recognizing urban shrinkage and growth patterns from a global  
729 perspective. *Applied Geography* **166**, 103247 (2024).
- 730 51. Does financial development increase energy consumption? The role of industrialization and  
731 urbanization in Tunisia. *Energy Policy* **40**, 473–479 (2012).
- 732 52. Pang, Y., Zhang, W. & Jiang, H. A socio-spatial exploration of rural livability satisfaction in  
733 megacity Beijing, China. *Ecological Indicators* **158**, 111368 (2024).
- 734 53. Tripathi, S. How does urbanization affect the human development index? A cross-country  
735 analysis. *Asia-Pac J Reg Sci* **5**, 1053–1080 (2021).
- 736 54. Mahendra, A. *et al.* Seven transformations for more equitable and sustainable cities. (2021).

- 737 55. Lima, M. F. & Eischeid, M. R. Shrinking cities: rethinking landscape in depopulating urban  
738 contexts. *Landscape Research* **42**, 691–698 (2017).
- 739 56. Zasada, I. *et al.* International retirement migration in the Alicante region, Spain: process, spatial  
740 pattern and environmental impacts. *Journal of Environmental Planning and Management* **53**,  
741 125–141 (2010).
- 742 57. Yu, L., Wang, Y. & Li, M. The emergence of counter-urbanisation in China: Can it be a pathway  
743 for rural revitalisation? *Habitat International* **144**, 102998 (2024).
- 744 58. Rasambainarivo, F. *et al.* Prioritizing COVID-19 vaccination efforts and dose allocation within  
745 Madagascar. *BMC Public Health* **22**, 724 (2022).
- 746 59. Petherick, A. *et al.* A worldwide assessment of changes in adherence to COVID-19 protective  
747 behaviours and hypothesized pandemic fatigue. *Nat Hum Behav* **5**, 1145–1160 (2021).
- 748 60. Shi, Y. *et al.* Lockdown policy in pandemics: Enforcement, adherence, and effectiveness in the  
749 case of COVID-19. *Infectious Disease Modelling* **10**, 493–504 (2025).
- 750 61. Nikiforiadis, A. *et al.* Exploring mobility pattern changes between before, during and after  
751 COVID-19 lockdown periods for young adults. *Cities* **125**, 103662 (2022).
- 752 62. World Population Review. Facebook Users by Country 2023.  
753 <https://worldpopulationreview.com/country-rankings/facebook-users-by-country> (2023).
- 754 63. Schiavina, M., Freire, S., Carioli, A. & MacManus, K. GHS-POP R2023A - GHS population grid  
755 multitemporal (1975-2030). European Commission, Joint Research Centre (JRC)  
756 <https://doi.org/10.2905/2FF68A52-5B5B-4A22-8F40-C41DA8332CFE> (2023).
- 757 64. Roskams, M. Population and household estimates, England and Wales: Census 2021. *Office for*  
758 *National Statistics* (2022).
- 759 65. Office for National Statistics (ONS). *Origin-Destination Data, England and Wales: Census 2021*.  
760 [https://www.ons.gov.uk/peoplepopulationandcommunity/populationandmigration/populationestimates/bulletins/origindestinationdataenglandandwales/census2021#origin-destination-](https://www.ons.gov.uk/peoplepopulationandcommunity/populationandmigration/populationestimates/bulletins/origindestinationdataenglandandwales/census2021#origin-destination-migration-data)  
761 [migration-data](https://www.ons.gov.uk/peoplepopulationandcommunity/populationandmigration/populationestimates/bulletins/origindestinationdataenglandandwales/census2021#origin-destination-migration-data) (2023).  
762

- 763 66. Ribeiro, F. N., Benevenuto, F. & Zagheni, E. How Biased is the Population of Facebook Users?  
764 Comparing the Demographics of Facebook Users with Census Data to Generate Correction  
765 Factors. in *Proceedings of the 12th ACM Conference on Web Science* 325–334 (Association for  
766 Computing Machinery, New York, NY, USA, 2020). doi:10.1145/3394231.3397923.
- 767 67. Li, Z., Ning, H., Jing, F. & Lessani, M. N. Understanding the bias of mobile location data across  
768 spatial scales and over time: A comprehensive analysis of SafeGraph data in the United States.  
769 *PLOS ONE* **19**, e0294430 (2024).
- 770 68. Bing Maps Tile System - Bing Maps. [https://learn.microsoft.com/en-us/bingmaps/articles/bing-](https://learn.microsoft.com/en-us/bingmaps/articles/bing-maps-tile-system)  
771 [maps-tile-system](https://learn.microsoft.com/en-us/bingmaps/articles/bing-maps-tile-system) (2022).
- 772 69. WorldPop. Global High Resolution Population Denominators Project - Funded by The Bill and  
773 Melinda Gates Foundation (OPP1134076). (2020) doi:10.5258/SOTON/WP00660.
- 774 70. Reia, S. M., Rao, P. S. C., Barthelemy, M. & Ukkusuri, S. V. Spatial structure of city population  
775 growth. *Nat Commun* **13**, 5931 (2022).
- 776 71. Milusheva, S., Björkegren, D. & Viotti, L. Can We Trust Smartphone Mobility Estimates in Low-  
777 Income Countries. *World Bank Blogs* [https://blogs.worldbank.org/en/opendata/can-we-trust-](https://blogs.worldbank.org/en/opendata/can-we-trust-smartphone-mobility-estimates-low-income-countries)  
778 [smartphone-mobility-estimates-low-income-countries](https://blogs.worldbank.org/en/opendata/can-we-trust-smartphone-mobility-estimates-low-income-countries) (2021).
- 779 72. Karra, K. *et al.* Global land use / land cover with Sentinel 2 and deep learning. in *2021 IEEE*  
780 *International Geoscience and Remote Sensing Symposium IGARSS* 4704–4707 (2021).  
781 doi:10.1109/IGARSS47720.2021.9553499.
- 782 73. Verbesselt, J., Hyndman, R., Newnham, G. & Culvenor, D. Detecting trend and seasonal changes  
783 in satellite image time series. *Remote Sensing of Environment* **114**, 106–115 (2010).
- 784 74. McKenzie, G. & Adams, B. A country comparison of place-based activity response to COVID-19  
785 policies. *Applied Geography* **125**, 102363 (2020).
- 786 75. Cleveland, R. B., Cleveland, W. S., McRae, J. E. & Terpenning, I. STL: A seasonal-trend  
787 decomposition. *Journal of Official Statistics* **6**, 3–73 (1990).

- 788 76. Boulton, C. A., Lenton, T. M. & Boers, N. Pronounced loss of Amazon rainforest resilience since  
789 the early 2000s. *Nat. Clim. Chang.* **12**, 271–278 (2022).
- 790 77. Woods, D. *et al.* Exploring methods for mapping seasonal population changes using mobile  
791 phone data. *Humanit Soc Sci Commun* **9**, 1–17 (2022).
- 792 78. Zeileis, A. A unified approach to structural change tests based on ML scores, F statistics, and OLS  
793 residuals. *Econometric Reviews* **24**, 445–466 (2005).
- 794 79. Bai, J. & Perron, P. Computation and analysis of multiple structural change models. *Journal of*  
795 *applied econometrics* **18**, 1–22 (2003).
- 796 80. Yu, C. & Yao, W. Robust linear regression: A review and comparison. *Communications in*  
797 *Statistics - Simulation and Computation* **46**, 6261–6282 (2017).
- 798 81. Bürkner, P.-C. brms: An R Package for Bayesian Multilevel Models Using Stan. *Journal of*  
799 *Statistical Software* **80**, 1–28 (2017).
- 800 82. Bonett, D. G. vcmeta: Varying Coefficient Meta-Analysis. 1.4.0  
801 <https://doi.org/10.32614/CRAN.package.vcmeta> (2021).
- 802 83. Grünwald, J., Hanzelka, J., Voříšek, P. & Reif, J. Long-term population trends of 48 urban bird  
803 species correspond between urban and rural areas. *iScience* **27**, 109717 (2024).
- 804 84. Hicks, D. A. The inequality-adjusted human development index: A constructive proposal. *World*  
805 *Development* **25**, 1283–1298 (1997).
- 806 85. Solt, F. Measuring Income Inequality Across Countries and Over Time: The Standardized World  
807 Income Inequality Database. *Social Science Quarterly* **101**, 1183–1199 (2020).
- 808 86. Wan, G., Zhang, X. & Zhao, M. Urbanization can help reduce income inequality. *npj Urban*  
809 *Sustain* **2**, 1 (2022).
- 810 87. Xu, H. & Jiao, M. City size, industrial structure and urbanization quality—A case study of the  
811 Yangtze River Delta urban agglomeration in China. *Land Use Policy* **111**, 105735 (2021).
- 812 88. Borck, R., Pflüger, M. & Wrede, M. A simple theory of industry location and residence choice.  
813 *Journal of economic geography* **10**, 913–940 (2010).

- 814 89. Mitchell, C. J. A. Making sense of counterurbanization. *Journal of Rural Studies* **20**, 15–34 (2004).
- 815 90. Hofstede, G. Country comparison. *Hofstede insights* (2018).
- 816 91. Tang, S. S., Zhou, J. & Liu, Y. Emerging in-migration of urban young adults engaging in rural  
817 tourism in China. *Population, Space and Place* **30**, e2791 (2024).
- 818 92. Oishi, S. The Psychology of Residential Mobility: Implications for the Self, Social Relationships,  
819 and Well-Being. *Perspect Psychol Sci* **5**, 5–21 (2010).
- 820 93. Chen, Z. & Paudel, K. P. Economic openness, government efficiency, and urbanization. *Review of*  
821 *Development Economics* **25**, 1351–1372 (2021).
- 822 94. Vehtari, A. *et al.* loo: Efficient leave-one-out cross-validation and WAIC for Bayesian models. (*No*  
823 *Title*) (2015).
- 824